

# <sup>99</sup>Tc NMR AND QUANTUM CHEMICAL STUDY OF THE CUBIC NANOPARTICLES OF Tc AND Tc-Ru ALLOYS SUPPORTED AT THE CERAMIC MATRIX SURFACES

K. E. German\*, Yu.V. Plekhanov\*, N. N. Popova\*<sup>1</sup>,  
V. P. Tarasov\*\*, Yu. B. Muravlev\*\*

\* Institute of Physical Chemistry, Russian Academy  
of Sciences, Leninskii pr. 31, Moscow, Russia

\*\* Kurnakov Institute of General and Inorganic Chemistry,  
Russian Academy of Sciences, Leninskii pr. 31, Moscow, Russia

Bulk Tc metal has an hcp lattice with  $a = 2.735$  and  $c/a = 1.6047$  while Tc films less than 150 Å thick are characterized by a fcc lattice with  $a = 3.68$  Å [1, 2]. Bulk Ru metal has a hcp lattice with  $a = 2.704$  Å and  $c/a = 1.5809$  and Tc–Ru alloys are infinite solid solutions [3]. NMR experimental parameters reflecting the metal electronic state and structure are the Knight isotropic shift ( $K$ ), its anisotropy ( $K_{an}$ ), spin–lattice relaxation time ( $T_1$ ), line width ( $\Delta\nu$ ), quadrupole coupling constant ( $C_Q$ ), and asymmetry parameter  $\eta$  of the electric field gradient tensor. We have recently determined these parameters for a Tc metal powder with a grain size of 50–100 μm:  $K = 6872$  ppm,  $K_{an} = -400$  ppm,  $(T_1 \times T)^{-1} = 3.23$  s<sup>-1</sup> K<sup>-1</sup>,  $C_Q = 5.74$  MHz, and  $\eta = 0$  [4]. For the bulk Ru metal at 4.2 K, the Knight shift is 4900 ppm [5]. Here, we present the results of studying Tc and Tc-Ru nanoparticles at ceramic surfaces by <sup>99</sup>Tc NMR. These mono-, bi- and polymetallic particles are interesting for their catalytic properties [1] and also for their segregation from oxide phase in spent nuclear fuel (into ε-phase). Three types of supports with basic properties were used, namely, γ-Al<sub>2</sub>O<sub>3</sub> (spinel, sp.surface 189 m<sup>2</sup>/g, pore size 320 and 40 Å), MgO (fcc, 46 m<sup>2</sup>/g, 20 Å) and TiO<sub>2</sub> (60% rutile+40% anatase, 7 m<sup>2</sup>/g, -). The dispersity and particle size of Tc metal were determined on an EM-301 transmitting electron microscope with a resolution of 3.5 Å [6]. The bar diagrams of size distribution of particles indicate that on a γ-Al<sub>2</sub>O<sub>3</sub> support with the highest specific surface, the size of Tc particles ranges from 10 to 80 Å (the average particle size is 23 Å for a 1% Tc/Al<sub>2</sub>O<sub>3</sub> catalyst) (Fig.1). This distribution is skewed toward larger particles with an increase in Tc concentration. For the MgO and TiO<sub>2</sub> supports with a smaller specific surface, size distribution is wider, the average particle size being above 40 Å. Tc and Tc-Ru nanoparticles were prepared by procedures described elsewhere [6]: support samples were impregnated with an aqueous solutions of NH<sub>4</sub>TcO<sub>4</sub> and RuCl<sub>3</sub>·H<sub>2</sub>O, dried at 80–90°C, and reduced in a hydrogen flow for 2–12 h at 700°C. The calculated amount of the deposited metal was ~0.01–20 wt % for Tc and 1–10 wt % for Ru. Samples (0.7–0.8 g) were placed in Teflon tubes (DxH=10x30 mm) for recording NMR spectra. <sup>99</sup>Tc NMR spectra were recorded at 293 K on a Bruker MSL-300 spectrometer in a magnetic field of 7.04 T at a frequency of 67.55 MHz.

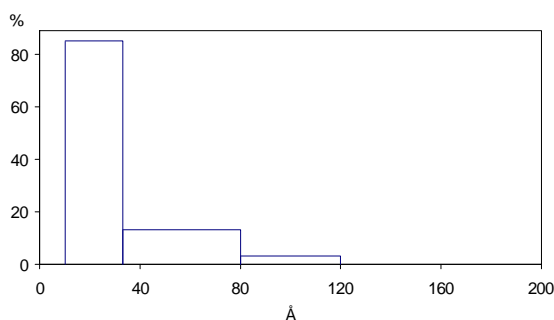


**Fig.1.** Approximate size distribution of Tc particles determined from TEM micrograph in the sample 1 % Tc/γ-Al<sub>2</sub>O<sub>3</sub>

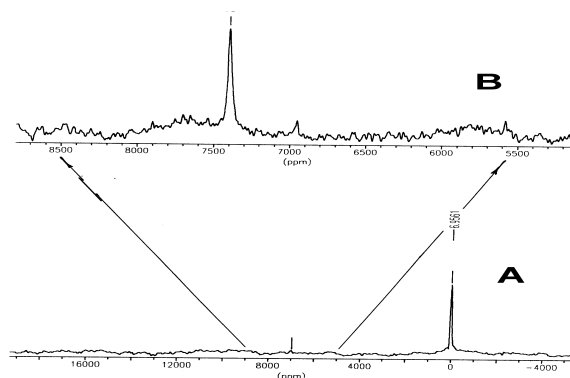


**Fig 2.** <sup>99</sup>Tc NMR spectra of a 5% Tc/γ-Al<sub>2</sub>O<sub>3</sub> catalyst at 295 K; (a) SW 1.7 MHz, NS 250000, (b) SW 250 kHz, NS 64000

<sup>1</sup> Present address : Vernadskiy Geochemistry and Analytical Chemistry Institute of Russian Academy of Sciences.

The spin echo pulse sequence was used. The width of the first exciting pulse was 3.22  $\mu\text{s}$ , repetition time was 0.5 s, and the number of scans was 64000 to 250000. The spin-lattice relaxation time  $T_1(^{99}\text{Tc})$  was measured using the saturation–recovery technique. The dependence of the peak amplitude of an NMR signal on the delay time is described by a one-exponential function. At 295K, the  $T_1$  is equal to 204 ms, which is about 200 times larger than that for the bulk metal [4]. Chemical shifts were referenced to a 0.1 M  $\text{KTcO}_4$  solution as the external standard. Support samples were spherical grains 1.5–2.0 mm in diameter. Spectra of reference  $\text{TcO}_2$  was recorded, indicating the signal characteristic of hexacoordinated Tc with 15 ppm chemical shift.  $^{99}\text{Tc}$  NMR spectra of all the Tc and Tc-Ru nanoparticles showed signals in the region of Tc metal shifts ( $\sim 7000$  ppm) and in the region of the external standard ( $\sim 10$  ppm) (due to surface oxidation to  $\text{TcO}_2$ ) (Fig. 2). The integrated intensity of the low-field signal that arose from Tc metal was roughly one order of magnitude weaker than the intensity of the  $\text{TcO}_2$  signal. The stronger signal from small particles has a shift of 7400 ppm. The weaker signal from large particles has a shift of about 6950 ppm. The  $^{99}\text{Tc}$  NMR shift and line shape for nanoparticles differ considerably from those for the bulk Tc sample (Fig.4). The shift is 7406 ppm, which is about 600 ppm larger than the shift for the bulk sample. The line with a width at half-maximum of  $\sim 1$  kHz has the Lorentzian shape and lacks the satellite structure caused by first-order quadrupole interactions, typical of the hexagonal close-packed lattice. The missing quadrupole structure clearly points to the cubic lattice of the nascent Tc phase. The increase in the Knight shift reflects a change in the density of states at the Fermi level, compared to the bulk Tc sample with the hexagonal close-packed lattice [4]. Figure 5 shows the temperature dependence  $K(T)$  of Knight shifts for the bulk sample and Tc nanoparticles.

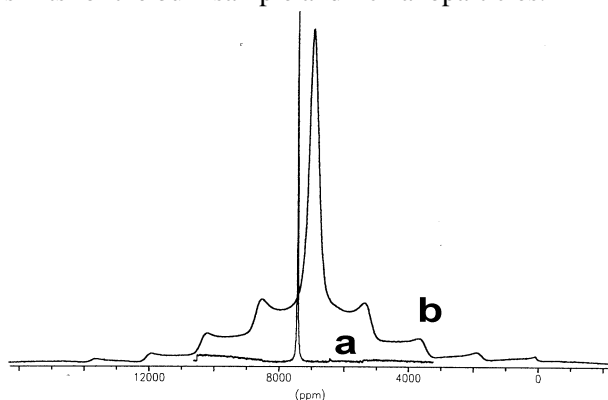


**Fig 4.**  $^{99}\text{Tc}$  NMR spectra of a (a) 20% Tc/ $\gamma$ -  $\text{Al}_2\text{O}_3$  catalyst at 295 K; SW 500 kHz, NS 191000,  $D_0$  0.5s; (b) bulk Tc metal, SW 2.5 MHz, NS 50000,  $D_0$  0.5s.

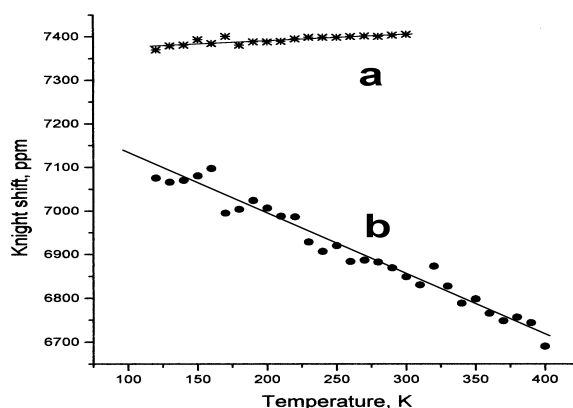


**Fig 5.** Temperature dependence of the Knight shifts at (a) 20% Tc/ $\gamma$ -  $\text{Al}_2\text{O}_3$  catalyst; (b) bulk Tc metal.

Compared to the  $K(T) = 7268 - 1.35T$  for the bulk sample, the temperature dependence of the Knight shift for nanoparticles is noticeably weaker,  $K(T) = 7360 + 0.16T$ , and has the opposite sign. Table 1 presents the measured  $^{99}\text{Tc}$  NMR parameters.

Table1.  $^{99}\text{Tc}$ -NMR parameters for  $\gamma$ - $\text{Al}_2\text{O}_3$  supported monometallic Tc catalysts

Tc content, %	Annealing time at 700°C, h	NMR shift, ppm		NMR line width, Hz $\pm 5\%$		Integrated intensity ratio Tc/ $\text{TcO}_2$
		Tc metal $K \pm 1.8$	$\text{TcO}_2$ $\delta \pm 0.2$	Tc metal	$\text{TcO}_2$	
0.05	12	7411.7	3.6	1215.9	1015.1	1/7
0.1	12	7411.7	3.1	1361.8	898.0	1/4
2	6	7411.7	1.3	1848.2	1443.9	1/12
5	12	7409.9	0.2	1653.6	1287.8	1/6
10	6	7409.9	1.6	1365.7	771.2	1/10
20	2	7408.1	0.9	960	878.3	1/8

This data shows that in all the samples Tc metal has a cubic structure. The line widths for the metal and TcO<sub>2</sub> are 1–5 kHz. The high content of TcO<sub>2</sub> in the samples points to the incomplete reduction of the initial salt to the metal or its back oxidation.

The <sup>99</sup>Tc NMR line shape for nanoparticles is represented by an asymmetric contour with a small shoulder at the high-field wing. The degree of asymmetry and the change in line width depend on the Tc concentration and annealing time of the catalyst. However, these changes are irregular (Table 1). We assumed that the <sup>99</sup>Tc NMR line is a composite one because of the size effects of nanoparticles and decomposed this line into components. Simulation of a contour with the LineSim program resulted in five components of the experimental line shape for the 2% Tc/Al<sub>2</sub>O<sub>3</sub> catalyst, in eight components for the bimetallic (3% Tc–1% Ru)/TiO<sub>2</sub> catalyst and seven components for the 10%Tc-10%Ru/γ-Al<sub>2</sub>O<sub>3</sub> catalyst. Each of the components has a Lorentzian shape and a width of 0.5–1.0 kHz. The area under a component corresponds to the relative concentration of a definite Tc metal form. Table 5 shows the results for two Tc–Ru catalysts and a 3%Tc–3%Pt/MgO catalyst.

As can be seen, neither the type of support nor the nature of the second metal has a little effect on the <sup>99</sup>Tc NMR line width and shift. This may be an indication of the absence of any intermetallic compounds in the catalysts studied.

Table 2. <sup>99</sup>Tc-NMR parameters for γ-Al<sub>2</sub>O<sub>3</sub> and TiO<sub>2</sub> supported bimetallic Tc catalysts

[Tc], %	Annealing time at 700°C, h	NMR shift, ppm		NMR line width, Hz ± 5%		Integrated intensity ratio Tc/TcO <sub>2</sub>	
		Tc metal K ± 1.8	TcO <sub>2</sub> δ ± 0.2	Tc metal	TcO <sub>2</sub>		
10	6	for 10% Ru – 10%Tc on γ-Al <sub>2</sub> O <sub>3</sub>					1/4.5
		7410.2	0.9	2075.2	1281.7		
3	2	for 1% Ru – 3%Tc on TiO <sub>2</sub>					1/4.6
		7395.5	-15.2	4263.8	3118.5		
3	12	for 3% Pt – 3%Tc on MgO					1/13
		7399.4	-11.7	3440.0	4018.5		

For the binary (3% Tc–1% Ru)/TiO<sub>2</sub> and 10%Tc-10%Ru/γ-Al<sub>2</sub>O<sub>3</sub>, the experimental line shape points to the multicomponent character of the signal.

A possible reason for this observation may be the narrower individual lines due to dilution of Tc with ruthenium. Since the width of each individual line is determined by dipole–dipole interaction between the magnetic moments of Tc spins, substituting Ru, characterized by low natural abundances of magnetic isotopes with small magnetic moments, for a fraction of Tc will lead to line narrowing.

The main parameters that determine the value of Knight shift are the electron density ρ<sub>n</sub> at the nucleus and density of states at Fermi level N(E<sub>f</sub>). Taking no account of relativistic effect in DV Xα code [7], we considered more adequate to use average valence electron density ρ<sub>vn</sub> at the nucleus. Both ρ<sub>vn</sub> and N(E<sub>f</sub>) were by approx. 10% higher for *hcp* clusters compared to *fcc* in good agreement with the observed Knight shifts.

## REFERENCES

1. Spitsin, V.I., Kuzina, A.F., Pirogova, G.N. *Itogi Nauki Tekh., Ser.: Neorg. Khim.*, 1984, vol. 10.
2. Golyanov, V.M., Elesin, L.A., Mikheeva, N.M., *Zh. Eksp. Teor. Fiz.*, 1973, vol. 18, p. 572.
3. Zaitseva, L.L., Velichko, A.V., Vinogradov, I.V., *Itogi Nauki Tekh., Ser. : Neorg. Khim.*, 1984, vol. 9.
4. Tarasov, V.P., Muravlev, Yu.B., Guerman, K.E., *J. Phys.: Condens. Matter* 2001, vol. 13, p. 11041.
5. Burgstaller A., Ebert H., Voitlander J. // *Hyperfine Interactions*, 1986, vol. 89, p. 1015
6. Pirogova, G.N., Popova, N.N., Voronin, Yu.V., *et al.*, *Zh. Fiz. Khim.*, 1990, vol. 64, no. 11, p. 2933.
7. Plekhanov Yu.V., German K. E., Sekine R. *This issue* (Proceedings of 3-d Russian-Japanese Seminar, 2002, Dubna, JINR, Russia).